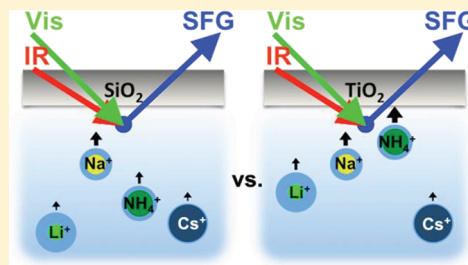


The Effects of Hofmeister Cations at Negatively Charged Hydrophilic Surfaces

Sarah C. Flores, Jaibir Kherb, Nicole Konelick, Xin Chen, and Paul S. Cremer*

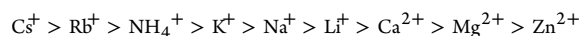
Department of Chemistry, Texas A&M University, College Station, Texas 77843, United States

ABSTRACT: This work explores the interactions of cations with highly negatively charged solid/aqueous interfaces. Vibrational sum frequency spectroscopy (VSFS) was exploited to observe interfacial water structure on the surfaces of fused quartz and titanium dioxide (TiO_2) in the presence of nine chloride salts with different alkali, alkaline earth, and transition metal cations. The results showed prominent specific cation effects at low concentration. The cations followed a direct Hofmeister series. On quartz surfaces the series was: $\text{Li}^+ > \text{Cs}^+ > \text{Rb}^+ > \text{NH}_4^+ > \text{K}^+ > \text{Na}^+ > \text{Ca}^{2+} > \text{Mg}^{2+} > \text{Zn}^{2+}$. As such, Zn^{2+} attenuated water structure to the greatest degree and therefore gave rise to the smallest peaks in the OH stretch region of the VSFS spectrum. The opposite was the case for Li^+ . Such results indicate that Li^+ partitioned least to the surface, while Zn^{2+} partitioned there to the greatest extent. We also observed prominent specific cation effects on TiO_2 surfaces. There were, however, some key differences between these surfaces. On TiO_2 , Li^+ , which is the best hydrated monovalent cation, behaved more similarly to K^+ and Na^+ . In addition, the ordering of Mg^{2+} and Ca^{2+} was reversed on TiO_2 compared with quartz. Such reordering of the Hofmeister series should result from differences in the charge density, polarizability, and basicity of the two oxide surfaces. Finally, NH_4^+ was found to interact more strongly with TiO_2 than any other monovalent cation. This result is in line with the greater role that hydrogen bonding should play on TiO_2 compared with quartz under the conditions of the experiment.



INTRODUCTION

The Hofmeister series involves the specific effects of ions in solution and was originally related to the solubility of proteins.^{1,2} Franz Hofmeister ranked anions and cations according to their ability to “salt in” or “salt out” proteins from aqueous solutions.³ For cations, the usual ordering of the series is:



The ions on the left tend to stabilize the native folded structure of a protein and decrease its solubility, while the ions on the right tend to facilitate protein denaturation and increase solubility.⁴ The effects of anions tend to be more pronounced than those of cations at relatively hydrophobic interfaces such as protein surfaces and therefore are easier to monitor.^{5–8} Generally speaking, there are fewer experimental studies exploring the interactions of cations.^{9–11}

Previously in our laboratory, vibrational sum frequency spectroscopy (VSFS) was used to observe the effects of anions by analyzing changes in the overall intensity of the water signal at the air/water interface in the presence of poly(*N*-isopropylacrylamide), bovine serum albumin, and surfactants.^{7,12} It was demonstrated that, for sufficiently charged macromolecules, the interaction with anions is electrostatic in nature and is dominated by the net charge of the monolayer rather than its detailed chemical structure. By analogy, it should be possible to observe changes in the intensity of the VSFS water spectrum at the solid/liquid interface in the presence of cations. Such data should provide important clues about

specific ion interactions with hydrophilic and negatively charged surfaces. Specifically, we provide a systematic study on the interactions of fused quartz and TiO_2 surfaces with various alkali, alkaline earth, and transition metal cations. The general setup is shown in Figure 1. Our observations provide clear evidence of the significance of the interactions between cations and negatively charged surfaces. The interactions vary with the intrinsic properties of the substrates as well as the physical nature of the individual cations. By choosing relatively simple systems such as quartz and TiO_2 , one can isolate predominantly electrostatic interactions from other factors such as hydrophobic interactions and structural complexity. The results may aid in understanding the mechanisms by which Hofmeister cations interact with more chemically complex systems such as peptides and proteins.

Inorganic cations and hydrophilic surfaces such as quartz and TiO_2 are not only good model systems for studying the Hofmeister series^{13–15} but are also of practical importance due to their relevance in processes like quartz dissolution, chemical polishing for the manufacturing of piezoelectric devices, sensor design, separations, and tribology.^{16–22} For example, it has been commonly observed that smaller monovalent cations such as Li^+ and Na^+ lead to higher dissolution rates of the substrate.^{17,18} Studies performed to model hydrothermal environments for geological and environmental applications have correlated an ion's adsorption strength to the silica surface with its ability to

Received: November 9, 2011

Revised: February 1, 2012

Published: February 28, 2012



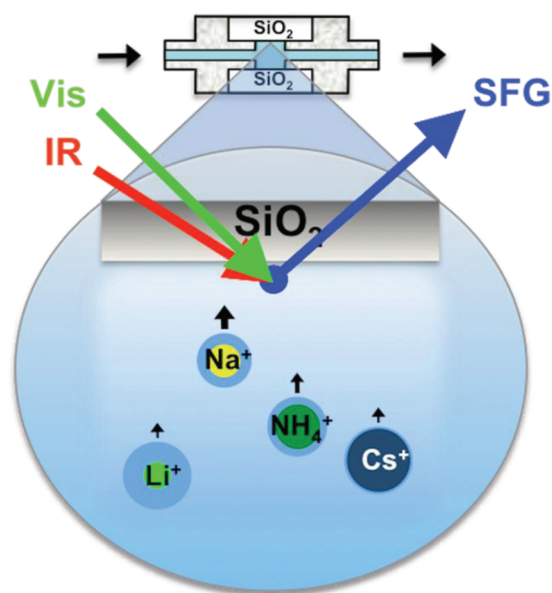


Figure 1. Schematic diagram of the flow cell for VSFS experiments at the solid/liquid interface with a fused quartz substrate.

accelerate quartz dissolution.²³ As such, a better understanding of cation–oxide interactions may help provide a molecular level understanding of the dissolution process of silica and other oxides.^{24–26}

EXPERIMENTAL METHODS

VSFS Experiments. VSFS is based on a nonlinear optical phenomenon, sum frequency generation (SFG), in which two photons are combined to generate a third. The frequency of the generated photon is the sum of the frequencies of the photons from the two incident beams.²⁷ In our experiments, one of the photons comes from an infrared source and the other from a visible beam. The probability of obtaining a sum frequency response is significantly enhanced when the frequency of the infrared beam is on resonance with specific molecular vibrations of the sample. Also, the sum frequency response is proportional to the intensities of the infrared and visible beams. In the dipole approximation,²⁷ the SFG response can only be obtained from media lacking inversion symmetry. Such unique selection rules guarantee the surface specificity of the technique. A more detailed explanation of the theoretical background^{28,29} and applications^{30,31} can be found in previous publications.

Our VSFS experimental setup consists of a 17-ps pulsed 1064 nm Nd:YAG laser (50 mJ; rate 20 Hz; Continuum, Santa Clara, CA), which pumps an optical parametric generator/amplifier (OPG/OPA, LaserVision, Bellevue, WA). The OPG/OPA system generates an infrared beam, which can be tuned between 2000 and 4000 cm^{-1} , supplying ~ 0.6 mJ per pulse in the CH and OH stretch region. The visible beam is fixed at 532 cm^{-1} (second harmonic of the fundamental) with ~ 1.0 mJ per pulse at the sample surface. The visible and infrared beams were spatially and temporally aligned at the solid/liquid interface, and the sum frequency response was recorded using a photomultiplier tube (Hamamatsu, Japan).

To perform VSFS experiments, quartz and TiO_2 -coated quartz substrates were placed inside a homemade Teflon flow cell as illustrated in the upper portion of Figure 1. The

fabrication of the flow cell has been previously described in detail.³²

Preparation of Hydrophilic Surfaces. IR grade quartz discs (1 in. diameter by $\frac{1}{8}$ in. thick; Quartz Plus Inc. Brookline, NH) were cleaned by the following standard procedure.³³ In brief, the quartz discs were immersed in piranha solution, followed by oven calcination, and subsequent immersion in concentrated sulfuric acid to obtain a hydrophilic, hydroxylated surface.

The cleaned quartz discs were used as substrates to grow TiO_2 thin films. The surfaces were prepared by evaporating titanium(IV) isopropoxide (97% $\text{Ti}(\text{OiPr})_4$, Aldrich, Milwaukee, WI) onto the quartz substrate for 10 min, which allowed the compound to react with surface silanol groups.³³ Finally, oven calcination was performed at 500 $^\circ\text{C}$ in order to oxidize the organic precursor into thin films of TiO_2 . These substrates were then employed in VSFS experiments. Such films have been previously characterized in our laboratory by X-ray photoelectron spectroscopy (XPS), atomic force microscopy (AFM), and ellipsometry to elucidate their elemental composition, roughness, and thickness.³³ These same measurements were reproduced for the samples used in this study in order to confirm the presence and properties of the TiO_2 thin films. The films had thicknesses of ~ 1.0 nm, which show very little nonresonant response. It should be noted that films generated in this way could be classified as neither anatase nor rutile but rather as an amorphous combination of the two. VSFS was used to further characterize the films in contact with an aqueous solution. The presence of an isoelectric point near pH 5.5 could be demonstrated by a minimum in the VSFS water structure at that pH value (data not shown). At pH 10.0, the water molecules should orient with their hydrogen atoms facing toward the negatively charged surface. Their orientation inverts as the pH is tuned below pH 5.5 because the surface becomes positively charged.³⁴

Preparation of Salt Solutions. Salt solutions were prepared in deionized water obtained from a Millipore filtration system (18M Ω ·cm; NANOpure Ultrapure Water System, Barnstead, Dubuque, IA) by dissolving the appropriate amount of high purity inorganic salt to form 0.10 M stock solutions of ZnCl_2 , MgCl_2 , CaCl_2 , LiCl , NaCl , KCl , NH_4Cl , RbCl , and CsCl (99+% Sigma-Aldrich Co.). Lower concentration salt solutions were prepared for VSFS experiments by further diluting the stock solutions to 0.033–1.00 mM. The concentrations of MgCl_2 , CaCl_2 , and ZnCl_2 were typically employed at one-third of those chosen for the monovalent cations in order to match the ionic strength between the monovalent and divalent systems. It should be noted that the selected range of salt concentrations was sufficient to perturb the water structure at the solid/liquid interface³⁵ and was the optimal for observing differences in water structure caused by the varying cations. It is important to point out that Zn^{2+} was only studied at a concentration of 0.033 mM. Under these conditions, the solubility product, which involves formation of zinc hydroxide, can be neglected.^{36,37} As such, the effects of Zn^{2+} in the present experiments were due to cation adsorption to the surface rather than changes in the pH of the bulk solution.

The pH was adjusted to 10.0 by using NaOH, which corresponds to a total NaOH concentration of 0.10 mM. This pH value is well above the pH values for the isoelectric points of the quartz and TiO_2 surfaces.^{38,33} It was chosen to maximize the amount of deprotonated OH surface groups, while keeping the background salt concentration reasonably low. It should be

noted that in the present experiments there was always a 0.10 mM background of Na^+ from the base, which also contributed to the apparent cation effects, in addition to the cation of interest. This concentration of Na^+ was kept constant in all cases; therefore, the differences observed in the VSFS water spectra reflect the specific cation effects for the different salts.³⁹

RESULTS

Figure 2A shows the VSFS spectrum of water (light blue data points) in contact with amorphous quartz at pH 10.0. The OH

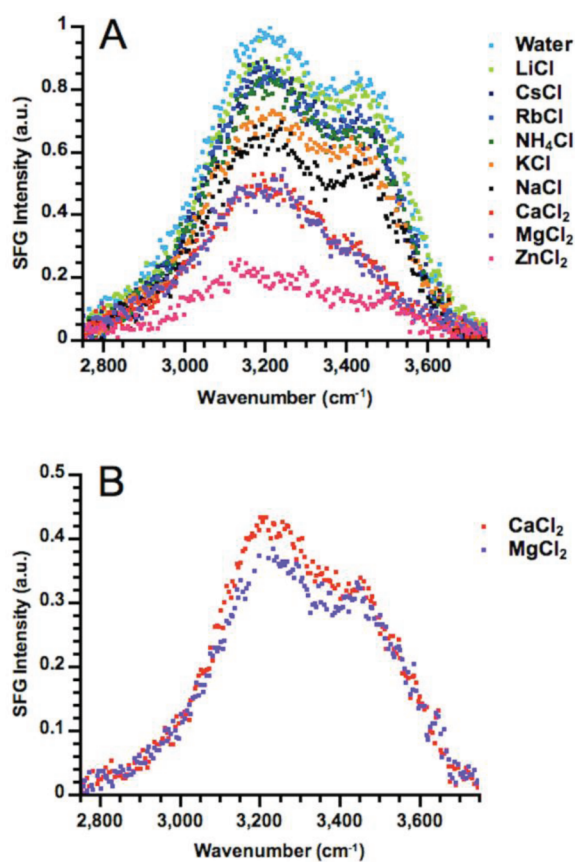


Figure 2. (A) VSFS spectra of the quartz surface at pH 10.0 in contact with 0.10 mM monovalent chloride salt solutions. The salt concentration was 0.033 mM for the divalent cations. (B) VSFS spectra of quartz surfaces at pH 10.0 in contact with 1.0 mM chloride salt solutions containing Ca^{2+} and Mg^{2+} .

stretch features near $\sim 3200\text{ cm}^{-1}$ and $\sim 3450\text{ cm}^{-1}$ reflect better coordinated and less coordinated water structure, respectively.²⁹ The water spectrum in the absence of additional salt gives rise to the highest VSFS intensity due to its lower ionic strength, which indicates the smallest charge screening effects in this case. VSFS results are also shown for the quartz surface in contact with nine chloride salt solutions at the same pH. The salt solution spectra demonstrate that the intensity for the water structure is attenuated in a cation-specific fashion. The decrease of VSFS signal reflects the extent of the interaction of each cation with the quartz surface, which leads to partial neutralization of the negative charge by the positively charged ions as well as through screening effects. The intensity of the water peaks follows a direct Hofmeister series. Specifically, divalent cations like Zn^{2+} adsorb preferentially to the solid surface, followed by Mg^{2+} and Ca^{2+} , then by the

monovalent cations Na^+ , K^+ , NH_4^+ , Rb^+ , Cs^+ , and Li^+ . In addition, the spectra for the divalent cations were obtained at 1.0 mM salt concentration (Figure 2B), which was found to be the optimal concentration for observing differences between Mg^{2+} and Ca^{2+} . As can be seen in Figure 2B, Mg^{2+} attenuates the water signal more strongly than Ca^{2+} .

Next, control experiments were performed in the absence of 0.1 mM NaOH. Under these conditions, the aqueous solutions were near neutral pH, and the quartz/water interface was significantly less deprotonated. As can be seen in Figure 3,

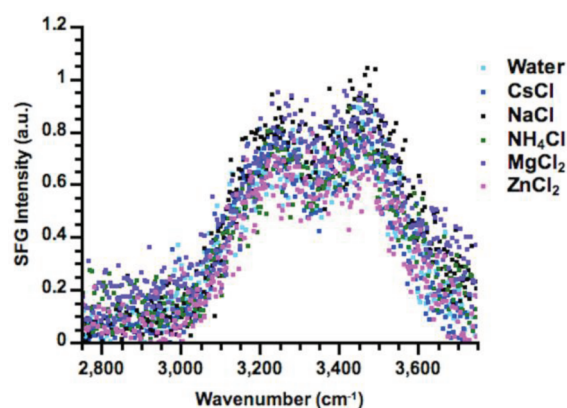


Figure 3. VSFS spectra of the quartz/water interface with 0.10 mM monovalent chloride salts and 0.033 mM divalent chloride salts. The nominal pH of these freshly prepared solutions was approximately 6.5.

addition of 0.033 mM divalent and 0.10 mM monovalent chloride salts to this system had a much less pronounced effect on the water structure, and any ion-specific differences were close to the limit of the experimental error. Such a result indicates that a negatively charged surface is critical to the differential attraction of the various Hofmeister cations.

Figure 4A shows VSFS data of the TiO_2 /aqueous interface with 0.1 mM monovalent and 0.033 mM divalent chloride salts at pH 10.0. These conditions match those employed at the quartz/water interface (Figure 2A). In this case, one observes much less pronounced differences between Ca^{2+} and Mg^{2+} . However, Zn^{2+} still appears to attenuate the water signal slightly more strongly than the other divalent cations. It also becomes difficult to discern the differences among NH_4^+ , K^+ , Na^+ , and Li^+ . However, at 0.33 mM divalent and 1.0 mM monovalent chloride salts, the spectra clearly reveal differences for the interactions of the cations with the surface (Figure 4B). In this case, Ca^{2+} attenuated the water signal more greatly than Mg^{2+} , followed by the monovalent cations NH_4^+ , Na^+ , K^+ , Li^+ , Rb^+ , and Cs^+ , in the given order.

DISCUSSION

Deprotonated OH groups at oxide surfaces are a key factor in determining the extent of cation adsorption and double layer screening, since the oxygen is the putative interaction site for cationic species. Both TiO_2 and quartz become more negatively charged as the pH is raised, and unsurprisingly, the adsorption of cations is favored at higher pH.^{40,41} For these oxides, there are obvious differences in the trends for interfacial cation partitioning as seen in Figures 2 and 4. This may be related to the basicity and polarizability of the surface sites.

The adsorption of cations on quartz surfaces at high pH generally follows a direct Hofmeister series with the exception

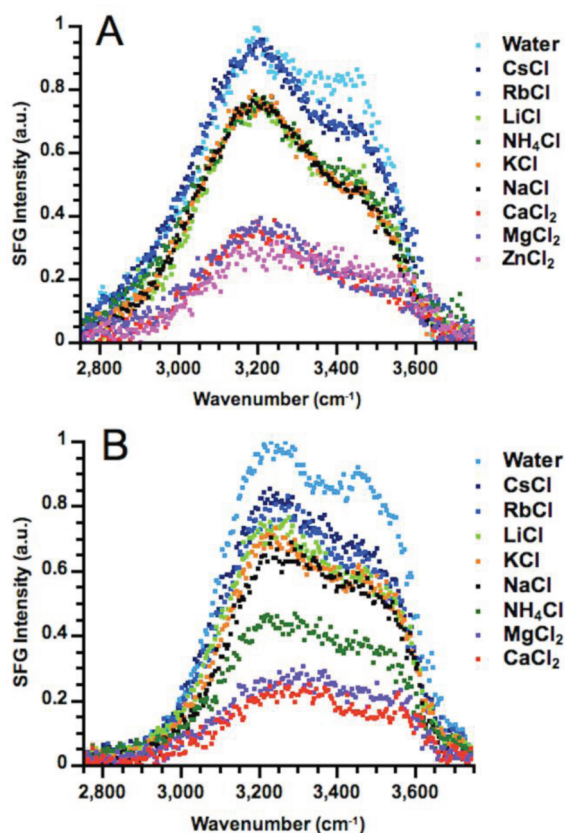


Figure 4. (A) VSFS spectra for TiO_2 surfaces at pH 10.0 in contact with 0.10 mM monovalent and 0.033 mM divalent chloride salt solutions. (B) VSFS spectra of TiO_2 surfaces at pH 10.0 in contact with 1.0 mM monovalent and 0.33 mM divalent chloride salt solutions.

of Li^+ . The adsorption is related to the size, net charge, and charge density of the ions (Figure 2). The divalent and smaller monovalent cations have a higher charge density than larger monovalent cations.^{42,10} Among the divalent ions, Zn^{2+} and Mg^{2+} are very similar in size. The observed difference in adsorption between them should be related to their relative affinities for the deprotonated surface silanol moieties. By analogy with hydroxide, the hydrolysis equilibrium constant value (K_1) for $\text{Zn}(\text{OH})^+$ is larger than that for $\text{Mg}(\text{OH})^+$.⁴³ In other words, Zn^{2+} forms tighter complexes with hydroxide. The solubility products (K_{sp}) in alkaline solutions for the three divalent cations used in this study follow the order $\text{Zn}^{2+} < \text{Mg}^{2+} < \text{Ca}^{2+}$.^{36,37} Therefore, a divalent cation's propensity for surface adsorption at the quartz/water interface to the silanol species appears to be in line with its propensity for complexation with hydroxide anions. Moreover, this same ordering has also been observed for the divalent cations with similar hydrophilic substrates like mica.⁴⁴

The series for monovalent cations is Na^+ , K^+ , NH_4^+ , Rb^+ , Cs^+ , and Li^+ on quartz, which mostly corresponds to a decreasing charge density trend. Strikingly, Li^+ is a strong exception. In fact, it behaves like an ion of even lower charge density than Cs^+ and Rb^+ . Indeed, Li^+ is known to be strongly hydrated in aqueous solutions.^{45–50} As such, the water molecules within the first hydration shell are tightly bound to the cation. The effective charge density for Li^+ is decreased by its hydration water and the surrounding water molecules become more polarized.⁵⁰ Phenomenologically, it appears to behave like a large cation with low charge density for various

systems. For example, similar anomalous behavior for Li^+ has been predicted by simulations at the air/water interface.⁵¹

Key differences between quartz and TiO_2 involve the dielectric constant and polarizability of the two substrates. TiO_2 , which is a semiconductor, has a much larger dielectric constant and is more polarizable than quartz.^{52,53} The isoelectric points of the two surfaces in aqueous solution are also quite different, pH 5.5 and pH 2.0, for TiO_2 and quartz, respectively.^{33,38} Therefore, cation adsorption on these substrates is expected to be somewhat different. Like quartz, the interactions of cations with TiO_2 still follow the same general trend based upon an ion's net charge. Indeed, divalent cations adsorb preferentially compared to monovalent cations. However, two metal cations, Li^+ and Ca^{2+} , show distinct behavior on TiO_2 compared with quartz (Figure 4B). On TiO_2 , Li^+ behaves in a fashion which is intermediate between Rb^+ and K^+ . Similarly, Ca^{2+} and Mg^{2+} switch places in the Hofmeister series on TiO_2 as compared with quartz. Thus, the properties of the substrate appear to be a crucial factor in the Hofmeister ordering of cation. Specifically, the more polarizable substrate, TiO_2 , shows greater deviations from the most commonly observed Hofmeister ordering. Such distinct properties may be important for biomaterials containing TiO_2 . Indeed, the preferential interaction of ions on this surface is believed to favor osteoblast development, bone growth, and protein adsorption on implants made of titanium, which typically has a thin TiO_2 coating in vivo.^{54–58}

Next, it should be noted that the position of NH_4^+ in the Hofmeister series with TiO_2 is also significantly shifted compared with quartz. In fact, it adsorbs more strongly than any other monovalent cation onto this substrate (Figure 4B). This behavior deviates from the expected Hofmeister series and may be related to the increased ability of TiO_2 to serve as a hydrogen bond acceptor. As noted above, TiO_2 is a more basic oxide than quartz. Because of the greater electropositive nature of the Ti atom compared with the Si atom, the oxygen atoms in TiO_2 are more electronegative and more likely to form hydrogen bonds with hydrogen bond donors like NH_4^+ ions.⁵⁹ Therefore, the adsorption of NH_4^+ on TiO_2 is not only dictated by its charge density but also by its hydrogen bonding ability.⁶⁰ It should be noted that NH_3 is also present in the solutions in contact with quartz and TiO_2 .³⁹ However, since this molecule does not bear a positive charge, it should have far less influence on the 3200 cm^{-1} peak in the SFG spectrum, which is closely related to the interfacial electric field strength. Moreover, NH_4^+ should accumulate at the negatively charged oxide interface to a much greater extent than the neutral NH_3 on electrostatic grounds. This idea agrees with calculated values of the adsorption energies of these two species.⁶⁰ Also, proton donation from NH_4^+ is more facile than from NH_3 , making such adsorption even more favorable to the TiO_2 surface.⁶⁰

In summary, the effects of Zn^{2+} , Mg^{2+} , Ca^{2+} , NH_4^+ , Li^+ , Na^+ , K^+ , Rb^+ , and Cs^+ ions on the water structure adjacent to negatively charged solid surfaces have been explored using VSFS at the oxide/aqueous interface. It was observed that at pH 10.0 and 0.033–1.0 mM salt concentrations the effects of the cations on the interfacial water structure were ion specific and followed an ordering mostly related to the charge density. Specific ion effects were less pronounced on less negatively charged surfaces. For both quartz and TiO_2 , the results demonstrated that the interactions of cations followed a direct Hofmeister series with a greater number of exceptions on TiO_2 than on quartz. The divergence in the ordering of the cations

on TiO₂ may be explained by the electronic properties, charge density, and hydrogen bonding ability of the substrates. Such insights may help provide information about how cations interact with more complex biological systems.

AUTHOR INFORMATION

Corresponding Author

*E-mail: cremer@mail.chem.tamu.edu. Phone: 979-862-1200.

Notes

The authors declare no competing financial interest.

ACKNOWLEDGMENTS

We thank the National Science Foundation (CHE-0094332) and the Robert A. Welch Foundation (Grant A-1421) for funding. Additionally, S.C.F. acknowledges CONACYT (Consejo Nacional de Ciencia y Tecnología) for Scholarship No. 210738.

REFERENCES

- (1) Kunz, W. *Curr. Opin. Colloid Interface Sci.* **2010**, *15*, 34.
- (2) Zhang, Y.; Cremer, P. S. *Curr. Opin. Chem. Biol.* **2006**, *10*, 658.
- (3) Hofmeister, F. *Arch. Exp. Pathol. Pharmacol.* **1888**, *24*, 247.
- (4) Kunz, W.; Henle, J.; Ninham, B. W. *Curr. Opin. Colloid Interface Sci.* **2004**, *9*, 19.
- (5) Cho, Y.; Zhang, Y.; Christensen, T.; Sagle, L. B.; Chilkoti, A.; Cremer, P. S. *J. Phys. Chem. B* **2008**, *112*, 13765.
- (6) Zhang, Y.; Cremer, P. S. *Proc. Natl. Acad. Sci.* **2009**, *106*, 15249.
- (7) Chen, X.; Flores, S. C.; Lim, S.-M.; Zhang, Y.; Yang, T.; Kherb, J.; Cremer, P. S. *Langmuir* **2010**, *26*, 16447.
- (8) Tobias, D. J.; Hemminger, J. C. *Science* **2008**, *319*, 1197.
- (9) Pegram, L. M.; Wendorff, T.; Erdmann, R.; Shkel, I.; Bellissimo, D.; Felitsky, D. J.; Record, M. T. Jr. *Proc. Natl. Acad. Sci.* **2010**, *107*, 7716.
- (10) Lo Nostro, P.; Frattini, L.; Ninham, B. W.; Baglioni, P. *Biomacromolecules* **2002**, *3*, 1217.
- (11) Klasczyk, B.; Knecht, V.; Lipowsky, R.; Dimova, R. *Langmuir* **2010**, *26*, 18951.
- (12) Chen, X.; Yang, T.; Kataoka, S.; Cremer, P. S. *J. Am. Chem. Soc.* **2007**, *129*, 12272.
- (13) Salis, A.; Boström, M.; Medda, L.; Parsons, D. F.; Barse, B.; Monduzzi, M.; Ninham, B. W. *Langmuir* **2010**, *26*, 2484.
- (14) Dove, P. M.; Craven, C. M. *Geochim. Cosmochim. Acta* **2005**, *69*, 4963.
- (15) Malati, M. A. *Surf. Coat. Technol.* **1987**, *30*, 317.
- (16) Deleuze, M.; Goiffon, A.; Ibañez, A.; Philippot, E. *J. Solid State Chem.* **1995**, *118*, 254.
- (17) Deleuze, M.; Goiffon, A.; Ibañez, A.; Philippot, E. *J. Mater. Sci.* **1996**, *31*, 2123.
- (18) Moldovan, C.; Iosub, R.; Modreanu, M. *Int. J. Inorg. Mater.* **2001**, *3*, 1173.
- (19) Stux, A. M.; Meyer, G. J. *J. Fluor.* **2002**, *12*, 419.
- (20) Tani, K.; Kubojima, H. *Chromatographia* **1998**, *47*, 655.
- (21) Donose, B. B.; Vakarelski, I. U.; Higashitani, K. *Langmuir* **2005**, *21*, 1834.
- (22) Pashley, R. M. *J. Colloid Interface Sci.* **1981**, *83*, 531.
- (23) Dove, P. M.; Crerar, D. A. *Geochim. Cosmochim. Acta* **1990**, *54*, 955.
- (24) Ishikawa, K.; Yoshioka, T.; Sato, T.; Okuwaki, A. *Hydro-metallurgy* **1997**, *45*, 129.
- (25) Paige, C. R.; Kornicker, W. A.; Hileman, O. E. Jr. *J. Radioanal. Nucl. Chem.* **1992**, *159*, 37.
- (26) Farrow, J. B.; Horsley, R. R.; Meagher, L.; Warren, L. J. *J. Rheol.* **1989**, *33*, 1213.
- (27) Shen, Y. R. *The Principles of Nonlinear Optics*; John Wiley & Sons: New York, 1984.
- (28) Shen, Y. R. *Nature* **1989**, *337*, 519.
- (29) Du, Q.; Freysz, E.; Shen, Y. R. *Phys. Rev. Lett.* **1994**, *72*, 238.
- (30) Weidner, T.; Breen, N. F.; Kun, L.; Drobny, G. P.; Castner, D. G. *Proc. Natl. Acad. Sci.* **2010**, *107*, 13288.
- (31) Chen, X.; Clarke, M. L.; Wang, J.; Chen, Z. *Int. J. Mod. Phys. B* **2005**, *19*, 691.
- (32) Kim, J.; Kim, G.; Cremer, P. S. *Langmuir* **2001**, *17*, 7255.
- (33) Kataoka, S.; Gurau, M. C.; Albertorio, F.; Holden, M. A.; Lim, S.-M.; Yang, R. D.; Cremer, P. S. *Langmuir* **2004**, *20*, 1662.
- (34) Shen, Y. R. *Solid State Commun.* **1998**, *108*, 399.
- (35) Yang, Z.; Li, Q.; Chou, K. C. *J. Phys. Chem. C* **2009**, *113*, 8201.
- (36) Shkol'nikov, E. V. *Russ. J. Appl. Chem.* **2004**, *77*, 1255.
- (37) Packter, A. *Cryst. Res. Technol.* **1981**, *16*, 1273.
- (38) Iller, R. K. *The Surface Chemistry of Silica*, 30th ed.; John Wiley & Sons: New York, 1979.
- (39) Although the current study mainly concerns the effects of metal cations, NH₄⁺ was also employed. It should be noted that at pH 10.0 there is only 15% ammonium (NH₄⁺) in solution. The other 85% of the initially added cations are in the deprotonated form, ammonia (NH₃).
- (40) Loewenstein, L. M.; Mertens, P. W. *J. Electrochem. Soc.* **1998**, *145*, 2841.
- (41) Dugger, D. L.; Stanton, J. H.; Irby, B. N.; McConnell, B. L.; Cummings, W. W.; Maatman, R. W. *J. Phys. Chem.* **1964**, *68*, 757.
- (42) Collins, K. D. *Biophys. J.* **1997**, *72*, 65.
- (43) Burgess, J. *Ions in Solution: Basic Principles of Chemical Interactions*; Horwood Publishing Limited: Chichester, 1999.
- (44) Parsons, D. F.; Ninham, B. W. *Langmuir* **2010**, *26*, 6430.
- (45) Varma, S.; Rempe, S. B. *Biophys. Chem.* **2006**, *124*, 192.
- (46) Rudolph, W.; Brooker, M. H.; Pye, C. C. *J. Phys. Chem.* **1995**, *99*, 3793.
- (47) Wachter, W.; Fernández, S.; Buchner, R.; Hefter, G. *J. Phys. Chem. B* **2007**, *111*, 9010.
- (48) Ansell, S.; Barnes, A. C.; Mason, P. E.; Neilson, G. W.; Ramos, S. *Biophys. Chem.* **2006**, *124*, 171.
- (49) Lyubartsev, A. P.; Laasonen, K.; Laaksonen, A. *J. Chem. Phys.* **2001**, *114*, 3120.
- (50) Loeffler, H. H.; Rode, B. M. *J. Chem. Phys.* **2002**, *117*, 110.
- (51) Horinek, D.; Herz, A.; Vrbka, L.; Sedlmeier, F.; Mamatkulov, S. I.; Netz, R. R. *Chem. Phys. Lett.* **2009**, *479*, 173.
- (52) Goniakowski, J.; Bouette-Russo, S.; Noguera, C. *Surf. Sci.* **1993**, *284*, 315.
- (53) Noguera, C.; Goniakowski, J.; Bouette-Russo, S. *Surf. Sci.* **1993**, *287/288*, 188.
- (54) Kasemo, B. *J. Prosthet. Dent.* **1983**, *49*, 832.
- (55) Diebold, U. *Surf. Sci. Reports* **2003**, *48*, 53.
- (56) Nayab, S. N.; Jones, F. H.; Olsen, I. *Biomaterials* **2007**, *28*, 38.
- (57) Ellingsen, J. E. *Biomaterials* **1991**, *12*, 593.
- (58) Klinger, A.; Steinberg, D.; Kohavi, D.; Sela, M. N. *J. Biomed. Mater. Res.* **1997**, *36*, 387.
- (59) Fu, Q.; Wagner, T. *Surf. Sci. Reports* **2007**, *62*, 431.
- (60) Markovits, A.; Ahdjoudj, J.; Minot, C. *Surf. Sci.* **1996**, *365*, 649.